National Aeronautics and Space Administration

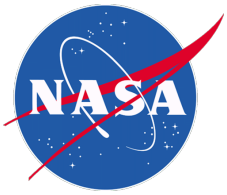

Algorithm Theoretical Basis Document (ATBD)
Version 06

NASA Global Precipitation Measurement (GPM) Integrated Multi-satellitE Retrievals for GPM (IMERG)

Prepared for:

Global Precipitation Measurement (GPM)
National Aeronautics and Space Administration (NASA)

Prepared by:

George J. Huffman
NASA/GSFC
NASA/GSFC Code 612
Greenbelt, MD 20771

and David T. Bolvin, Dan Braithwaite, Kuolin Hsu, Robert Joyce, Christopher Kidd, Eric J. Nelkin, Soroosh Sorooshian, Jackson Tan, Pingping Xie

13 March 2019

TABLE OF CONTENTS

LIST OF FIGURES

Page

LIST OF TABLES

Page

1. INTRODUCTION

1.1 OBJECTIVE

This document describes the algorithm and processing sequence for the Integrated Multi-satellitE Retrievals for GPM (IMERG). This algorithm is intended to intercalibrate, merge, and interpolate "all" satellite microwave precipitation estimates, together with microwave-calibrated infrared (IR) satellite estimates, precipitation gauge analyses, and potentially other precipitation estimators at fine time and space scales for the TRMM and GPM eras over the entire globe. The system is run several times for each observation time, first giving a quick estimate and successively providing better estimates as more data arrive. The final step uses monthly gauge data to create research-level products. Background information and references are provided to describe the context and the relation to other similar missions. Issues involved in understanding the accuracies obtained from the calculations are discussed. Throughout, the current Version 06 product is described, together with options and planned improvements that might be instituted in future version(s) depending on maturity and project constraints.

1.2 REVISION HISTORY

Version	*Date*	*Author*	*Description*
1.0	30 November 2010	G. Huffman	Initial version
2.0	30 November 2011	G. Huffman	Second delivery version
3.0	30 November 2012	G. Huffman	Third delivery version
3.1	12 July 2013	G. Huffman	Document Prob. Liq. Precip. Type
4	30 September 2013	G. Huffman	Fourth delivery version
4.1	16 December 2013	G. Huffman	At-launch modifications
4.2	20 December 2013	G. Huffman	Edits; add overpass diagram
4.3	22 July 2014	G. Huffman	Edits for post-launch information
4.4	15 September 2014	G. Huffman	Change to single snapshot each half hour
4.5	16 November 2015	G. Huffman	Version and Run file naming, current status, input satellite dates
4.6	14 March 2017	G. Huffman	Initial upgrade to GPM V05
5	9 November 2017	G. Huffman	Upgrade to IMERG V05
5.1	10 November 2017	G. Huffman	No GPROF-TMI; trimmed MHS, ATMS swaths
5.2	1 February 2018	G. Huffman	
6	13 March 2019	G. Huffman	Upgrade to IMERG V06

2. OBSERVING SYSTEMS

Historically and for the foreseeable future, passive microwave (PMW) sensors provide the lion's share of relatively accurate satellite-based precipitation estimates, and these are only available from low-Earth-orbit (leo) platforms. IMERG is designed to compensate for the limited sampling

available from single leo-satellites by using as many leo-satellites as possible, and then augmenting with geosynchronous-Earth-orbit (geo) infrared (IR) estimates. This happens in two ways. First, the leo-PMW data are morphed (linear interpolation following the estimated precipitation feature motion). Second, geo-IR precipitation estimates are included using a Kalman filter when the leo-PMW are too sparse. Additionally, precipitation gauge analyses are used to provide crucial regionalization and bias correction to the satellite estimates. None of the satellites except the GPM Core satellite are under GPM direction. Therefore, IMERG uses as many satellites of opportunity as possible in a very flexible framework. Table 1 gives a listing of the current and planned data sources, and the date spans of useful operation. Note that we plan to provide a continuous record from the beginning of TRMM. In all cases except the geo-IR and the precipitation gauge analyses the input data are accessed as Level 2 (scan-pixel) precipitation.

2.1 CORE SATELLITES

The TRMM satellite and GPM Core Observatory serve as both a calibration and an evaluation tool for all the PMW- and IR-based precipitation products integrated in IMERG in their respective eras, since they provide match-ups with all other PMW-equipped leo-satellites and IR-equipped geo-satellites. [Note that all of the PMW data are used to calibrate the IR estimates.] Both the TRMM and GPM satellites provide multi-channel, dual-polarization PMW sensors and active scanning radars. Three critical improvements in GPM are that 1) the orbital inclination has been increased from 35° to 65°, affording coverage of important additional climate zones; 2) the radar has been upgraded to two frequencies, adding sensitivity to light precipitation; and 3) "high-frequency" channels (165.5 and 183.3 GHz) have been included in the GPM Microwave Imager (GMI), which provide key information for sensing light and solid precipitation. The higher inclination for the GPM orbit reduces the radiometer and radar sampling compared to TRMM in the latitude band covered by TRMM.

2.2 MICROWAVE CONSTELLATION

The constellation of PMW satellites (Fig. 1) is largely composed of satellites of opportunity. That is, their orbital characteristics, operations, channel selections, and data policies are outside the control of NASA, with the exception of the GPM Core satellite. The imager channels are considered best for low- and mid-latitude use, while the sounding channels maintain some skill in cold and frozen-surface conditions.

2.3 IR CONSTELLATION

Although three different organizations control the geo-IR satellites, long-standing international agreements ensure coordination of orbits and mutual aid in the event of an unexpected satellite failure. The basic requirement is for full-disk images every three hours at the major synoptic times (00, 03, …, 21 UTC). All satellite operators provide a great deal of imagery beyond that, although piecing it together can be somewhat challenging. These data are accessed as brightness temperatures (Tb) in the merged format developed at NOAA/CPC for CMORPH. The dataset assembly is carried out at NOAA/CPC.

2.4 ADDITIONAL SATELLITES

Experience in creating fully global precipitation products for the Global Precipitation Climatology Project (GPCP) demonstrates that precipitation estimated from satellite soundings using the Susskind et al. (1997) algorithm has useful skill at scales as fine as 1° daily (Adler et al. 2003; Huffman et al. 1997). Even assuming that high-frequency channels on AMSU, ATMS, MHS,

GMI, and SSMIS eventually provide high-quality precipitation estimates at high latitudes, we expect that the cloud retrieval-based estimates may still be needed to fill gaps in the collection of high-latitude estimates. As well, CPC has shown some skill in using IR data from the Advanced Very High Resolution Radiometer (AVHRR) from low-orbit satellites for estimating precipitation at high latitudes.

Table 1. List of current and planned contributing data sets for IMERG, broken out by sensor type. Data sets with start dates of Jan 98 extend before that time, but these prior data are not used in IMERG. Square brackets ([ ]) indicate an estimated date. "M-T" stands for Megha-Tropiques. The M-T MADRAS instrument is not included on this list because of its short, gappy record. The geosynchronous IR data are processed into merged files at NESDIS. All data are at Level 2 (scan/pixel) except for the precipitation gauge analyses and IR data, which are at Level 3 (gridded). PPS maintains a list of anomalies in the microwave constellation sensors at ftp://gpmweb2.pps.eosdis.nasa.gov/tsdis/AB/docs/gpm_anomalous.html.

Merged Radar – Passive Microwave Imager Products	
Product	*Period of Record*
GPM DPR-GMI	Apr 14 - [Feb 24]
TRMM PR-TMI	Jan 98 - Sep 14

Conically-Scanning Passive Microwave Imagers and Imager/Sounders	
Sensor	*Period of Record*
Aqua AMSR-E	Jun 02 - Oct 11
DMSP F13 SSMI	Jan 98 - Nov 09
DMSP F14 SSMI	Jan 98 - Aug 08
DMSP F15 SSMI	Feb 00 - Aug 06
DMSP F16 SSMIS	Nov 05 - [Dec 19]
DMSP F17 SSMIS	Mar 08 - [Dec 20]
DMSP F18 SSMIS	Mar 10 - [Mar 20]
DMSP F19 SSMIS	Dec 14 – Feb 16
GCOMW1 AMSR2	Jul 12 - [May 22]
GOSAT-3 AMSR3	[Feb 22] - [Jan 32]
GPM GMI	Mar 14 - [Feb 24]
METOP-SG B1 MWI	[Jan 22] – [Dec 32]
METOP-SG B2 MWI	[Jan 29] – [Dec 39]
METOP-SG B3 MWI	[Jan 36] – [Dec 46]
TRMM TMI	Jan 98 – Apr 15
WSF-M 1 MIS	[Jan 22 – Jan 28]
WSF-M 2 MIS	[Jan 27 – Jan 33]

Table 1, continued.

Cross-Track-Scanning Passive Microwave Sounders	
Sensor	*Period of Record*
JPSS-2 ATMS **	[Jan 22] - [Jan 28]
JPSS-3 ATMS **	[Jan 26] - [Jan 32]
JPSS-4 ATMS **	[Jan 31] - [Jan 37]
METOP-2/A MHS **	Dec 06 - [Aug 22]
METOP-1/B MHS **	Apr 13 - [Aug 23]
METOP-3/C MHS	[Apr 19] - [Apr 27]
METOP-SG A1 MWS	[Jan 22] – [Dec 32]
METOP-SG A2 MWS	[Jan 29] – [Dec 39]
METOP-SG A3 MWS	[Jan 36] – [Dec 46]
M-T SAPHIR *	Oct 11 - [Jan 20]
NOAA-15 AMSU **	Jan 00 - Sep 10
NOAA-16 AMSU **	Oct 00 - Apr 10
NOAA-17 AMSU **	Jun 02 - Dec 09
NOAA-18 MHS **	May 05 – Oct 18
NOAA-19 MHS **	Feb 09 - [Apr 20]
NOAA-20 ATMS **	Nov 17 - [Aug 24]
SNPP ATMS **	Dec 11 - [Dec 19]

* Parts of the SAPHIR record suffer drop-outs. As well, the PRPS estimates do not provide estimates for the 5 footprints at each swath edge.

** The V06 GPROF estimates for AMSU, ATMS, and MHS do not provide estimates for the 5, 8, and 5 footprints (respectively) at each swath edge.

Geosynchronous Infrared Imagers		
Satellite	*Sub-sat. Lon.*	*Agency*
GMS, MTSat, Himawari series	140°E	JMA
GOES-E series	75°W	NESDIS
GOES-W series	135°W	NESDIS
Meteosat prime series	0°E	EUMETSAT
Meteosat repositioned series	63°E, from Jul 98 41°E, from Oct 16	EUMETSAT

IR/Passive Microwave Sounders		
Sensor	*Period of Record*	*Institution*
Aqua AIRS	Sep 02 - [Sep 20]	NASA/GSFC DISC
NOAA-14 TOVS	Jan 98 - April 05	Colo. State Univ.; NOAA/NCEI
NOAA-20 CrIS	[Nov 17 - Jun 22]	NASA/GSFC DISC
SNPP CrIS	[Nov 11 – [Nov 21]	NASA/GSFC DISC

Precipitation Gauge Analyses		
Analysis	*Period of Record*	*Institution*
Full Version 2018	Jan 98 – Dec 16	DWD/GPCC
Monitoring Version 6	Jan 17 - ongoing	DWD/GPCC

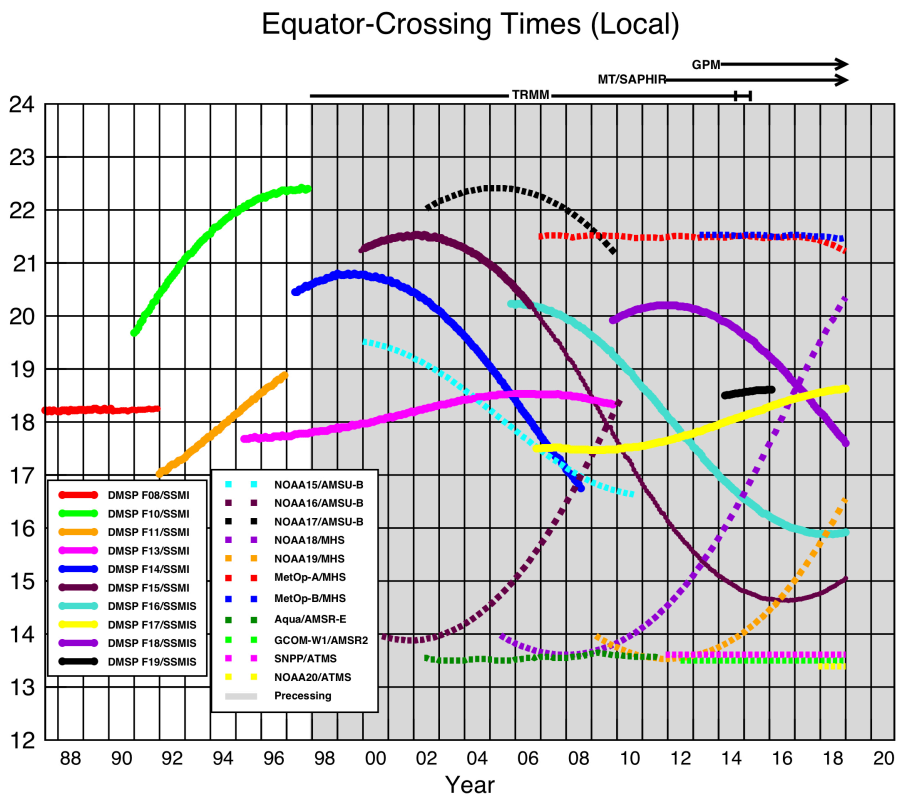

Ascending passes (F08 descending); satellites depicted above graph precess throughout the day.
Image by Eric Nelkin (SSAI), 30 January 2019, NASA/Goddard Space Flight Center, Greenbelt, MD.

Fig. 1 PMW sensor Equator-crossing times for 12-24 Local Time (LT; 00-12 LT is the same) for the modern PMW sensor era These are all ascending passes, except F08 is descending. Shading indicates that the precessing TRMM, Megha-Tropiques, and GPM cover all times of day. [Image by Eric Nelkin (SSAI; GSFC), 30 January 2019; https://pmm.nasa.gov/sites/default/files/imce/times_allsat.jpg holds the current version.]

2.5 PRECIPITATION GAUGES

Work in GPCP and TRMM has shown that incorporating a uniform precipitation gauge analysis is important for controlling the bias that typifies satellite precipitation estimates. These projects show that even monthly gauge analyses produce significant improvements, at least for some regions in some seasons. Recent work at CPC shows substantial improvements in the bias correction using daily gauge analysis for regions in which there is a sufficient number of gauges. It is planned to explore the use of daily gauges.

The Deutscher Wetterdienst (DWD) Global Precipitation Climatology Centre (GPCC) was established in 1989 to provide high-quality precipitation analyses over land based on conventional precipitation gauges. We use two GPCC products, the V8 Full Data Analysis for the majority of the time (currently 1998-2016), and the V6 Monitoring Product from 2017 to the then-present.

The Monitoring Product is posted about two months after the month of observation (see Becker et al. 2013; Schneider et al. 2014, 2018) and is based on SYNOP and monthly CLIMAT reports

received in near-real time via GTS from ~7,000–8,000 stations world-wide reported in the following sources:

- monthly precipitation totals accumulated at GPCC from the SYNOP reports received at DWD, Offenbach,
- monthly precipitation totals accumulated at NOAA/CPC from the SYNOP reports received at NOAA, Washington D.C.,
- monthly precipitation totals from CLIMAT reports received at DWD, Offenbach, Germany,
- monthly precipitation totals from CLIMAT reports received at the UK Met. Office (UKMO), Exeter, UK, and
- monthly precipitation totals from CLIMAT reports received at Japan Meteorological Agency (JMA), Tokyo, Japan.

GPCC's Full Data Analysis is based on a data base that covers the period 1901 up to 2013 (current V7 released in late 2015). Compared to the Monitoring Product, the Full Data Analysis includes additional data acquired from global data collections such as GHCN, FAO, CRU; data sets from the National Meteorological and/or Hydrological Services of about 190 countries of the world; and some data from GEWEX-related projects.

For both products, if data are available from more than one source for a station, an "optimum" value – according to the quality of the different data sources – is selected for the precipitation analysis. The selected precipitation data undergo an automatic pre-screening, and subsequently the data flagged as questionable are interactively reviewed by an expert. Based on the remaining quality-controlled station data, the (monthly) anomalies from the background climatology are computed at the stations, interpolated using the SPHEREMAP objective analysis, and added to the background climatology to create the month's analysis. Note that anomalies that are "too far" from any stations are set to zero to prevent unrealistic influence across vast distances.

CPC collects daily precipitation gauge data from ~16,000 stations around the world through the GTS, and from enhanced national networks over the U.S., Mexico, and a few other countries. They analyze global daily precipitation on a near-real-time basis by interpolating quality-controlled station reports. Note that the "day" in this analysis is defined region by region, not at a uniform UTC time. These data are the basis for the daily satellite-gauge option in Subsection 3.14.4.

Precipitation gauges suffer a variety of errors in collecting precipitation, including evaporation, splashing, side wetting, and wind effects, with all resulting in a low bias for most gauge configurations. The wind effects occur because the air has to flow around the opening of the gauge and hydrometeors tend to follow the air flow. This is most true for the hydrometeors that fall the most slowly, namely drizzle and snowflakes. Undercatch ranges from 5% in heavy rain situations to 100%, 200% or more, and depends on the design of the gauge (Legates 1987; Sevruk 1989). Until recently, the state of the art was a set of monthly maps of climatological adjustment ratios computed by Legates and Willmott (1990), and these are used to adjust the gauge analyses in this work. Recently, the GPCC has started computing daily adjustments based on station meteorological data for the Monitoring Analysis starting in 1982 (Schneider et al. 2014) based on Fuchs et al. (2001), and this will be studied for use in a future version of IMERG.

3. ALGORITHM DESCRIPTION

Given the available diverse, changing, uncoordinated set of input precipitation estimates, with various periods of record, regions of coverage, and sensor-specific strengths and limitations, we seek to compute the longest, most detailed record of "global" precipitation. To do this, we combine the input estimates into a "best" data set. Although we wish to maintain reasonable homogeneity in the input datasets, for example by using consistently processed archives for each sensor and undertaking multiple inter-calibrations, we are not striving to compute a Climate Data Record dataset.

The requirements for the multi-satellite product are summarized in Table 2. The space-time resolution is roughly the microwave spatial scale and the IR temporal scale. The space-time domain represents the PMM goal of covering the whole globe starting with TRMM. Multiple output products are specified to satisfy different classes of users, summarized in Subsection 3.2. The term "snapshot" for half-hourly estimates reflects the fact that individual satellite overpasses are the basis for these data and that the resulting satellite estimates are not "instantaneous", but represent an interval that can exceed an hour (Villarini et al. 2008). The best TRMM, and then GPM estimate of precipitation should be taken as the calibration standard. Currently this is considered to be the GPM Combined Radar-Radiometer (CORRA-G, using GMI and DPR), and an equivalent computation using TMI and PR during the TRMM era (CORRA-T), collectively referred to as CORRA. As well, gauge data are clearly important for anchoring the satellite estimates. Error estimates and auxiliary data fields included in the output files are key to giving users (and developers) the information needed to assess quality by time and region over the life of the dataset. Finally, as a quasi-operational system, the code must "take a licking and keep on ticking."

3.1 ALGORITHM OVERVIEW

A great deal of expertise in merged precipitation algorithms was developed in the U.S. during the TRMM era, funded mainly by PMM and by NASA NEWS, NOAA programs (CPO, USWRP), NSF SAHRA, and UNESCO G-WADI. IMERG drew on the strengths of the various groups on the PMM Science Team to create a unified U.S. algorithm. Specifics are:

- Perform careful intercalibration of microwave estimates
  - the GSFC group has a strong background
- Provide finer time and space scales to get adequate sampling
  - the CPC group has strong experience with quasi-Lagrangian time interpolation using Kalman filters – CMORPH-KF
- Provide microwave-calibrated IR estimates to fill "holes" in the PMW constellation
  - the CPC group operationally produces the 4-km Merged IR Tb products
  - the U.C.-Irvine group has strong experience in computing IR estimates
- Incorporate gauge data to control bias
  - the GSFC group has a strong background in monthly corrections
  - the CPC group has developed a test system to perform daily bias correction
- Provide error estimates
  - both the GSFC and CPC groups bring strengths
- Deliver and support a code package that runs in the PMM Precipitation Processing System (PPS) environment
  - the GSFC group has a strong track record

The high-level block diagram that results from this analysis is shown in Fig. 2, which identifies the institutions that provide the heritage code for the various blocks.

Table 2. Notional requirements for IMERG. CORRA refers to the Combined Radar Radiometer Analysis for both the TRMM and GPM eras.

Resolution	0.1° [i.e., roughly the resolution of microwave estimates]
Time interval	30 min. [i.e., the geo-satellite interval]
Spatial domain	global
Time domain	1998-present; later explore entire SSMI era (1987-present)
Product sequence	"Early" sat. (~4 hr), "Late" sat. (~14 hr), "Final" sat.-gauge (~3.5 months after month) [more data in longer-latency products]
Instantaneous vs. accumulated	Snapshot for half-hour, accumulation for monthly; data centers provide value-added products for other accumulation periods
Sensor precipitation products intercalibrated to CORRA	
Global, undercatch-adjusted monthly gauge analyses including retrospective product; explore use in submonthly-to-daily and near-real-time products	
Error estimates, including "quality"; final form still open for definition	
Embedded data fields showing how the estimates were computed	
Precipitation phase estimates; probability of liquid precipitation	
Operationally feasible, robust to data drop-outs and (constantly) changing constellation	
Output in HDF5 (compatible with NetCDF4); data centers provide value-added products for other formats, and with spatial and parameter subsetting	
Archiving and retrospective processing for all RT and post-RT products	

3.2 PROCESSING OUTLINE

3.2.1 Initial Processing

The block diagram for IMERG is shown in Fig. 2. In words, the input precipitation estimates computed from the various satellite PMW sensors are assembled, mostly received at PPS as Level 1 brightness temperatures from the relevant providers, converted to GPM Level 1C intercalibrated brightness temperatures, then converted to Level 2 precipitation estimates using GPROF2017 (currently). The single exception is that the SAPHIR data are not well-behaved in GPROF, so those data are processed using the Precipitation Retrieval and Profiling Scheme (PRPS; Kidd 2018). All estimates are gridded, intercalibrated to the CORRA product on a rolling 45-day basis using probability matching, and climatologically calibrated to the GPCP monthly estimates with a simple ratio in high latitude oceans (where CORRA V06 is deficient in precipitation) and over all land (where the CORRA tends to be high). These "high quality" (HQ) data are combined into half-hourly fields and provided to both the CPC Morphing-Kalman Filter (CMORPH-KF; Joyce et al. 2011) quasi-Lagrangian time interpolation scheme and the Precipitation Estimation from Remotely Sensed Information using Artificial Neural Networks – Cloud Classification System (PERSIANN-CCS; Hong et al., 2004) re-calibration scheme. In parallel, CPC assembles the zenith-angle-corrected, intercalibrated merged geo-IR fields and forwards them to PPS for use in the PERSIANN-CCS computation routines. In previous versions, the "displacement vectors" needed in the CMORPH-KF quasi-Lagrangian time interpolation scheme were computed from "even-odd" files of the IR data, also supplied by CPC. However, these vectors are now computed from Modern Era Retrospective Reanalysis 2 (MERRA-2) and Goddard Earth Observing System model (GEOS) Forward Processing (FP) data (Section 3.3.3), which PPS routinely ingests. The

PERSIANN-CCS estimates are computed (supported by an asynchronous re-calibration cycle) and sent to the CMORPH-KF quasi-Lagrangian time interpolation scheme. The CMORPH-KF quasi-Lagrangian time interpolation (supported by an asynchronous KF weights updating cycle) uses the PMW and IR estimates to create half-hourly estimates. Note that various intermediate fields are carried through the processing as necessary to populate the fields in the output file (Table 3).

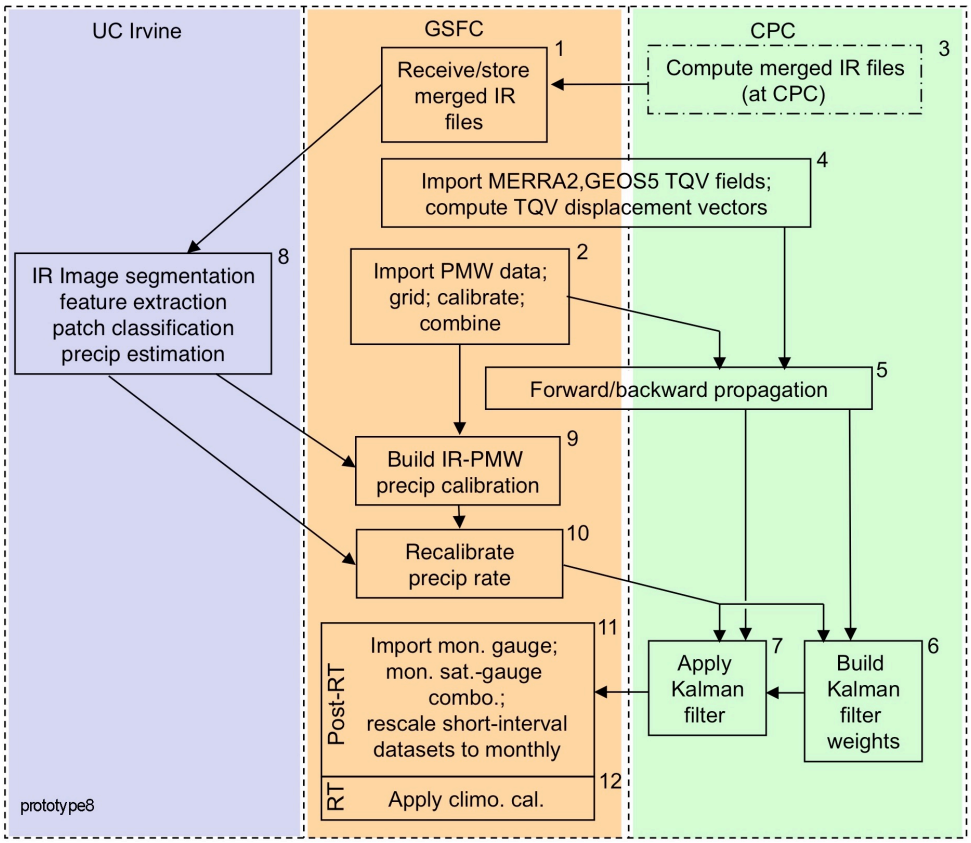

Fig. 2. High-level block diagram illustrating the major processing modules and data flows in IMERG. The blocks are organized by institution to indicate heritage, but the final code package is an integrated system. The numbers on the blocks are for reference in Section 5. Box 3 is computed at CPC as an integral part of IMERG.

Precipitation phase is computed in the microwave merger step as a diagnostic using surface type, surface pressure, surface temperature, and surface humidity (Section 3.10). The system is run twice in near-real time:

- "Early" multi-satellite product ~4 hr after observation time and
- "Late" multi-satellite product ~14 hr after observation time,

and once after the monthly gauge analysis is received

- "Final" satellite-gauge product ~3.5 months after the observation month.

The baseline is for the "Early" and "Late" half-hour estimates to be calibrated to the Final product with climatological coefficients that vary by month and location, while in the Final product the half-hour multi-satellite estimates are adjusted so that they sum to the monthly satellite-gauge combination computed in IMERG (following the TMPA approach). In all cases the output

contains multiple fields that provide information on the input data, selected intermediate fields, and estimation quality.

Given the multiplicity of runs discussed here and below, it is key to IMERG maintainability and consistency that all of the runs share a common code. The different runs are achieved with options programmed into the single system, even though PPS chooses to install separate instantiations of the code for each run.

Finally, the Early and Late runs are executed in the PPS Real Time (RT) processing system, which is keyed to rapid creation of results, while the Final run is executed in the PPS Production processing system.

3.2.2 Retrospective Processing

Retrospective processing is key to creating consistent archives of data for users. This is true for users of all three runs of IMERG, so all three are reprocessed. By design, the Production processing system, which computes the Final run, supports reprocessing. The RT processing system, which computes the Early and Late runs, does not support reprocessing. This issue is addressed by retrospectively processing IMERG in the Production system with calls that mimic the processing for Early and Late. Specifically, the selection of input data available to the retrospective Early Run will be approximated by limiting the forward time span of data to the typical latency time (~3 hours) before the Early run time (currently 4 hours after observation time). For simplicity, this solution is implemented by using Production input datasets. These choices cause the Early Run to be reprocessed with a superset of input data covering the original Early, and the input data from a particular sensor are produced by the "climo" GPROF estimates (computed with more-carefully prepared reanalysis data). In a future release we may decide to institute climatological calibrations in the retrospective Early Run that are different from those in the Early. The same is true for the Late setting a latency limit of ~11 hours.

Retrospective processing for both the Early and Late Runs is carried out after retrospective processing for the Final Run to allow computation of climatological calibration coefficients for Early and Late to the Final monthly product (which has gauge information). As well, this allows use of intermediate Final results already computed, shortening the processing cycle. This comes at the expense of using a superset of the data that actually were available in real time (i.e., also using data that came in after what would have been received in time for the original near-real-time computation), and perhaps some slightly different calibrations.

3.2.3 Rotating Calibration Files and Spin-Up Requirements

There are three calibrations that require routine rotating accumulators in IMERG. First, there is the primary calibration of precipitation products, which in the TRMM era is carried out as TMI calibrated to CORRA-T, and in the GPM era is carried out as GMI calibrated to CORRA-G. This calibration is done over an interval of 9 5-day periods (9 pentads) for stability. [Recall that the TMI and GMI products are used as calibrators for all the other satellite precipitation estimates. This is done because matchups between CORRA-T or CORRA-G with the other sensors are exceedingly sparse.] Note that TMI is reduced to the status of just another (high quality) sensor during the period in which GMI is officially operating. The rotating calibrations are necessarily trailing in the Early and Late runs, but we use a centered approach for the Final run.

The second rotating accumulator is for the Kalman filter, whose statistics are currently calibrated over a 3-month period. A side study showed that this interval yields results very similar to a 5-month period.

The third rotating accumulator is for the PERSIANN-CCS/PMW calibration, which uses an interval of 6 pentads (30 days) for stability. The accumulator file is trailing for the Early and Late runs and centered for the Final run.

There are also a number of calibrations that are currently climatological, but have the potential to be converted to rotating calibration files in the future if further research shows that the climatological approach is insufficiently accurate. These include the various calibrations of other sensor precipitation datasets to TMI and GMI in their respective eras.

The final issue for the rotating accumulation files is providing seed and restart files. The development team provides the start-of-record seed files for TRMM and GPM. Thereafter, in normal operations the rotating files are programmed to refresh as new data arrive. However, it is likely that processing difficulties, bad input data, or undetected code errors will force a restart of processing. To accommodate such cases, PPS saves daily dumps of rotating accumulation files and all the intermediate files.

3.3 INPUT DATA

3.3.1 Sensor Products

The sensor products are detailed in Section 2 as part of the discussion of the various sensors. For the most part, the datasets listed in Table 1 from previous and current sensors are already archived at PPS as part of the TMPA work under TRMM, but the requirement in GPM is that all inputs be processed using the current GPM version of GPROF2017. As such, we are working closely with the developers at Colorado State Univ. and with PPS in testing to ensure the best quality products.

Note that the V05 GPROF estimates for AMSU-B, ATMS, MHS, and SAPHIR do not provide estimates for the 5, 8, 5, and 5 footprints (respectively) at each swath edge. This is due to algorithm issues as revealed in early testing. Taken together, these limitations somewhat reduce the amount of microwave-based data contained in Version 06 IMERG. Future reprocessings will correct these issues.

3.3.2 Ancillary Products

The ancillary products required on a routine basis for the IMERG algorithm are surface type, surface pressure, surface temperature, and surface relative humidity. Surface type is provided by the standard static map of percent water coverage from PPS. Surface pressure, surface temperature, and surface relative humidity are provided by the JMA forecasts (for Early) and GANAL gridded assimilation (for Late) of meteorological data. The Final Run uses the ECMWF analysis for consistency with the "climatological" run of GPROF2017.

3.3.3 MERRA-2 and GEOS FP Products

MERRA-2 is a global atmospheric reanalysis beginning in 1980 using the EOS-5 data assimilation system and numerical model (Bosilovich et al. 2016; Gelaro et al 2017). GEOS FP is a global forecast analysis using the GEOS-5 system at every 6 hr (Lucchesi 2017). Both datasets are processed and released by the NASA Global Modeling and Assimilation Office.

The total precipitable water vapor (TQV; also called total column water vapor) is used in V06 to compute the displacement vectors for morphing the PMW data. In addition, the total precipitable liquid water (TQL), total precipitable ice water (TQI), and surface precipitation rate (PRECTOT) will be revisited in V07 for a role in computing the displacement vectors. PPS extracts all four data fields from daily files of hourly data at 0.5°x0.625° latitude/longitude for MERRA-2, and

from hourly files at 0.25°x0.3125° latitude/longitude for GEOS FP, feeding into post-real-time and retrospective processing, and near-real-time processing, respectively.

GEOS FP is episodically upgraded as research progresses. The IMERG team considers the impact of each such upgrade, but in general they are minor compared to the approximations involved in computing the displacement vectors.

3.3.4 GPCP SG Product

The GPCP is an international, community-based activity of the Global Energy and Water Exchange (GEWEX) project that produces long-term, global, climate-oriented precipitation datasets. The Satellite-Gauge (SG) product is a monthly analysis on a 2.5°x2.5° grid for 1979 to the present, delayed by about 3 months. It merges various satellite-based estimates over both ocean and land, combined with the precipitation gauge analyses over land from the GPCC. The satellite-based estimates are IR-based, calibrated by passive microwave estimates for the latitude band 40°N-S, passive microwave outside of that rolling over to IR/microwave sounders contributing at higher latitudes. The algorithm, currently at V2.3, is described in Adler et al. (2003, 2018) and prior paper referenced therein. A significant effort is made to enforce homogeneity on the input data sets and the resulting merged analysis across the span of the analysis. Where possible, this includes using an overlap time period to adjust for data and/or algorithm differences and to remove data source artifacts.

3.3.5 NOAA Autosnow Product

The NOAA Autosnow product is used to provide global data on daily surface coverage by snow and ice. Currently, information on the snow cover is derived from the Advanced Very High Resolution Radiometer (AVHRR) onboard METOP satellites, imagers onboard Geostationary Operational Environmental Satellites (GOES) East and West, Spinning Enhanced Visible and Infrared Imager (SEVIRI) onboard Meteosat second Generation (MSG), and Special Sensor Microwave Imager/Sounder (SSMIS) onboard Defense Meteorological Satellite Program (DMSP) satellites. Ice cover is derived from the METOP AVHRR and DMSP SSMIS data. Both snow and ice are identified in satellite images using threshold-based decision tree image classification algorithms. Information on snow and ice cover derived from observations in the visible/infrared and the microwave bands is combined to generate continuous (gap-free) maps on a daily basis. The main output product of the system is a daily global snow and ice cover map generated on a 0.04° lat/lon grid (Plate Carree), which is about 4x4 km at the Equator. See Romanov (2016) for more details.

The Autosnow product is used at two stages:

1. mask snow/ice surface in the computation of the Kalman statistics, and
2. mask the output IMERG precipitation estimates.

Currently IMERG uses all microwave estimates in the merge and propagation steps to allow for eventual global coverage when the microwave estimates have integrity over cold surface.

3.4 MICROWAVE INTERCALIBRATION

As with TMPA, the IMERG precipitation estimates are calibrated to the TRMM/GPM single- or combined-sensor estimates deemed highest-quality following Huffman et al. (2007), currently the CORRA estimates. During the initial release period in the GPM mission a short-record (6-9 month-based) calibrator was used, pending a longer GPM-based calibrator, while in V05 and V06 it is seasonal averages for 2015. The microwave intercalibration technique is based on quantile-quantile matching, similar to Miller (1972) and Krajewski and Smith (1991). The temporal and spatial scale of the histogram matching for any given sensor depends upon the unique orbit and individual sensor characteristics. Vastly different orbits, leading to fewer data overlaps, may require a longer calibration period to ensure representative geographic and diurnal sampling. Similarly, radically different sensors may require sampling at higher spatial and temporal resolution. Climatological (fixed, generally seasonally varying) calibrations are used when possible, with dynamically-computed (monthly, say) calibrations utilized when necessary.

The TMI- and GMI-CORRA calibrations are computed on a 1°x1° grid using a 3°x3° template. Experience in V03 showed that regions with differing gradients in GMI and CORRA resulted in blocky patterns when the calibrations were used on the original 1° grid. So, starting in V05, the calibrations used were distance-weighted interpolations of the four surrounding 1° calibration values.

The TMI- and GMI-other-satellite calibrations are computed on 22 15° zonal histogram bands overlapping at 5° increments for ocean. A single histogram is used for land due to sampling concerns. Experience in V03 showed that zonal bands with differing gradients between GMI and cross-track sounders occasionally resulted in zonal discontinuities when the calibrations were used on the center 15° band. So, the sounder calibrations are equal-weighted averages of the upper, center, and lower band calibration values. However, testing for V05 showed that high-rate grid boxes were badly overestimated in this process, so GMI-other-satellite calibrations were not carried out in V05 except for SSMIS, whose PDF of GPROF precipitation rates differed from the other constellation sensors. In V06, all constellation satellites are intercalibrated to TMI and GMI using the ocean and land histogram technique previously described. The cross-track scanners employ the equal-weighted average of the upper, center, and lower ocean band values but the along-track scanners do not. The results show that constellation satellite calibration to GMI was challenging due to the sampling as a result of the GPM orbit and the sun-synchronous satellite orbits. SSMIS was significantly overcorrected over land so it was decided to leave the SSMIS estimates as is. Due to sparse sampling, TMI was not calibrated to GMI and is used as is. Calibration of constellation satellites to TMI in the TRMM era proved more stable and all satellites are intercalibrated.

CMORPH-KF, PERSIANN-CCS, and TMPA-RT all use various lengths of trailing calibration in which updating is considered necessary, and this is the intended approach for the near-real-time IMERG Runs. The post-real-time TMPA uses a calendar-month calibration, but for consistency across the IMERG Runs, we routinely update the Final calibrations such that each day is approximately in the middle of the calibration period except for the Kalman statistics computation which is uses the current and two previous months so it is at the end of the calibration period.

One improvement in GPM over TRMM is that both DPR and CORRA-G are available in real time, whereas PR and TCI were not in TRMM. This allows us to have the same calibrating sensor for all the IMERG runs in Initial Processing (i.e., computations with newly received data).

Even though CORRA is considered to be the best estimator, in V06 (as in V04 and V05) all of the GPM individual-sensor precipitation products are biased low in the high latitude oceans compared to the GPCP Satellite-Gauge product and estimates based on CloudSat (Behrangi et al. 2014 and subsequent revisions to the approach). There is some variation between the latter two, but the GPCP can provide regionally varying monthly climatological adjustment factors, while the CloudSat-based data currently only have an annual latitudinal profile over ocean. Thus, in V06 (as in V04 and V05) we are making a simple ratio adjustment to bring the CORRA-calibrated constellation estimates in line with what is considered a more reasonable estimate. We apply these corrections outside of a somewhat subjectively chosen, seasonally varying low-latitude zone where the ratio of CORRA to GPCP is close to one. Meanwhile, over land the CORRA is frequently too high, so a seasonal calibration to GPCP is applied at all latitudes. This is not as severe as it first appears, since GPCP includes gauge data, and the complete IMERG products (for all Runs) include calibration to monthly gauge analyses, climatologically for Early and Late, and by month for Final. The same principle is applied in the TRMM era using TMI-CORRA. Finally, in the TRMM era the CORRA-T calibration must be extended out from 35°N and S to higher latitudes. In TMPA this was done with a smooth-fill, which proved to yield problematic results in the cold season, but now the extension can use the actual CORRA-G values to more closely approximate the extension. Calibration outside the CORRA-T area of coverage in the GPM era is provided by extrapolating the northernmost and southernmost CORRA-G correction curves at 60º N and S to the poles using a 50-pass iterative smooth-fill technique to obtained corrections in the latitude bands 60º-90º N and S. To add stability to the extrapolated correction curves, the zonal mean of the corrections is computed at 60º N and S and assigned to the 90º N and S zonal bands, respectively.

In the TRMM era, background monthly climatological GPM-era GMI-CORRA histograms and correction curves are used to fill in the corrections for the latitude bands 33º-90º N and S. This fill in is performed as follows:

1. Compute the count-normalized precipitation volumes for CORRA-G and CORRA-T in the latitude bands 0º-33º N and S using the TMI-CORRA month and GMI-CORRA background histograms.
2. Compute volume adjustment factors for northern and southern hemisphere ocean and land.
3. Apply these volume adjustment factors to the GPM background correction curves.
4. Insert the volume-adjusted GPM correction curves into the T-CORRA correction curves in the region 25º-90º N and S, performing a weighted average of the two corrections in the latitude bands 25º-33º N and S.

The resulting corrections are based on TRMM for the latitude band 25ºN-25ºS, volume-adjusted GPM for the latitude bands 33º-90º N and S, and a blend of the two in the latitude bands 25º-33º N and S. The goal is to provide the GPM correction structure outside the TRMM coverage area, but with the volume of the TRMM estimates. This was necessary, as directly extrapolating the TRMM region corrections to the poles created artificially low corrections.

3.5 MERGED MICROWAVE

The intercalibrated microwave precipitation estimates from GMI, TMI, and all of the partner sensors in the constellation are merged to create Level 3 data sets containing the best observational data available in each half hour. All of the input data sets are gridded from their native Level 2 swath data to the IMERG 0.1°x0.1° Level 3 global grid on the IMERG half-hourly interval (namely the first and second half hour for each UTC hour). The grid is populated with sensor data in the priority order conical-scan radiometer, and then cross-track scanner. [Note: this is a good choice over ocean, but not necessarily for land areas.] If there is more than one sensor in a class, the one

closer to the center of the half hour is chosen. The precipitation estimate, sensor type, and time of observation (to the nearest minute) are reported in the output data set. Starting with V05, the gridding was extended to fully global (90°N-S), and inserted into the merged microwave.

3.6 MICROWAVE-CALIBRATED IR

Geo-satellites give frequent sampling, but the resulting IR Tb data are related to cloud top features (temperature and albedo) rather than directly to surface precipitation. This indirect relationship is best captured if the IR Tb-precipitation relationship is improved using texture and patch classification as well as applying routine updates using leo-PMW based precipitation estimates. Here, following the PERSIANN-CCS (Hong et al. 2004), the 60°N-S latitude belt that contains geo-IR data is subsetted into 24 overlapping sub-regions (six in longitude by four in latitude) to allow for regional training and parallel processing. For each sub-region, the full-resolution IR Tb field is segmented into separable cloud patches using a watershed algorithm. Cloud patch features are extracted at three separate temperature levels: 220K, 235K, and 253K, which are chosen to represent the cloud patches at different altitudes in the atmosphere. [Expansion to a fourth, warmer threshold is underway to better capture precipitation from low clouds, particularly in dry zones.] An unsupervised clustering analysis (Self-Organizing Feature Map) is used to classify cloud patches into a number of cloud patch groups based on the similarities of patch features. Precipitation is assigned to each classified cloud patch group based on a training set of leo-PMW precipitation samples. These initial precipitation estimates are then dynamically calibrated to the HQ precipitation estimates using a 30-day calibration updated every pentad.

3.7 KALMAN-SMOOTHER TIME INTERPOLATION

Under the Kalman Smoother framework as developed in CMORPH-KF and applied here, the precipitation analysis for a grid box is defined in three steps (Joyce et al. 2011). First, PMW estimates of instantaneous rain rates closest to the target analysis time in both the forward and backward directions are propagated from their observation times to the analysis time using the cloud motion vectors computed from the TQV images (see next paragraph). The “prediction” of the precipitation analysis is then defined by compositing the forward- and backward-propagated PMW estimates with weights inversely proportional to their error variance. At this point the propagated fields are masked for surface snow and ice using Autosnow (Section 3.3.5) to account for the low skill of GPROF in quantitative precipitation retrieval in such conditions If the time interval from the nearest PMW observation is longer than 30 minutes, the final "analysis" is defined by updating the “forecast” with IR-based precipitation observations with weights inversely proportional to the observational correlations. This 30-minute threshold is due both to the natural timescale of precipitation at these fine scales and to the retrieval errors in the microwave algorithms. By about ±90 minutes the IR has higher correlation than the propagated microwave data.

Up through V05, the cloud motion vectors used to propagate the PMW estimates were calculated by computing the pattern correlation between spatially lagged geo-IR Tb arrays from two consecutive images. The spatial displacement with the highest correlation was used to define the cloud motion vector. The cloud motion vectors were defined for each 2.5° lat/lon grid box using IR data over a 5° lat/lon domain centered on the target grid box. Over mid-latitudes, precipitation systems present slightly different movements than the cloud systems that the geo-IR Tb depict. To account for the differences, Joyce et al. (2011) compared the PDFs of the zonal and meridional components of the cloud motion vectors against those of the precipitation systems observed by the Stage II radar over the contiguous U.S. (CONUS). A static correction table was then established

for adjusting the geo-IR-based cloud motion vectors in both hemispheres' mid-latitudes to better represent precipitation motion. Interpolation in time, and then space was used to provide spatially complete propagation fields.

In Fall 2017, it turned out that the "even-odd" files needed for the IR-based scheme were not available in a timely fashion for most of the TRMM era. Accordingly, the plan to explore use of numerical model data was put on the fast track. Previous work by P. Xie (CPC) showed some utility in this approach, although his particular implementation was less skillful than the IR-based system at low latitudes. The development effort at GSFC evaluated PRECTOT, TQI, TQL, and TQV, all of which are available in both MERRA-2 (for non-real-time use) and GEOS FP (for near-real-time use) at hourly native resolution. Summary statistics show that TQV generally has the highest scores (mostly by a small amount) over the other three, and is competitive with the IR. In fact, at most latitudes TQV outperforms IR and tends to avoid the IR's problem of mistaking high-level cirrus motion for the actual motion of the precipitation systems when they are shallow and embedded in a vertically sheared flow. An additional benefit of TQV is that it provides spatially complete fields of vectors, eliminating the time/space interpolations required by the intermittent results from the other fields. [Even though IR is complete except for occasional sector dropouts, it must be thresholded to mimic "cold" precipitating clouds, so the vector field has holes.] Finally, TQV (and the other numerical model fields) provide vectors at all latitudes, unlike the IR's limitation to 60°N-S (due to the viewing geometry of the geo-satellites). Because the TQV fields are hourly, the first half of each hour is given half of the hourly displacement field, and the second half of each hour is an interpolation between the adjacent first-half-hour values. As with IR, the motion vectors are calculated for each 2.5° lat/lon grid point over a 5° lat/lon domain, though the offset for each precipitation pixel is linearly interpolated to 0.1°x0.1° from the four closest vectors to improve fine-scale motion. See *https://pmm.nasa.gov/sites/default/files/document_files/MorphingInV06IMERG.pdf* for details.

Errors for the individual satellite estimates are calculated by comparison against TMI/GMI estimates. Error tables for the TMI/GMI are taken to be the same as those for the AMSR-E, based on an early comparison against the Stage II radar observations over CONUS. Expressed in the form of correlation, the errors for the propagated PMW estimates are defined as regionally dependent and seasonally changing functions of sensor type (imager, sounder, IR) and the length of propagation time. Over land, the error tables are computed for each 10° latitude band using data collected over a 30°-wide latitude band centered on the target band. No zonal differences in the error are considered due to the limited sampling of the data. Over ocean, the error tables are defined for each 20°x20° lat/lon box using data over a 60°x60° lat/lon region centered on the target box. Over both land and ocean, the error tables are calculated for each month using data over a three-month period, trailing for Early and Late, and trailing from the target month for Final, to account for the seasonal variations. The comparisons against Stage II were done once, while those against TMI/GMI are updated monthly.

3.8 SATELLITE-GAUGE COMBINATION

For the baseline post-real-time IMERG package, we follow the TMPA approach for infusing monthly gauge information into the fine-scale precipitation estimates (Huffman et al. 2007). All of the full-resolution half-hour multi-satellite estimates in a month are summed to create a monthly multi-satellite-only field. This field is combined with the monthly GPCC precipitation gauge analysis (over land) in a three-step process. First, the gauge analysis is adjusted for undercatch by multiplying the monthly precipitation values by the corresponding month's gridbox climatological adjustment ratios from Legates and Willmott (1990). Second, the multi-satellite estimate is

adjusted to the large-spatial-scale mean of the gauges, and finally, the adjusted multi-satellite and gauge fields are combined using weighting by inverse estimated error variance. This monthly satellite-gauge combination is a product in its own right (see Table 3). In addition, the field of ratios between the original monthly multi-satellite and monthly satellite-gauge fields is computed, then each field of multi-satellite precipitation estimates in the month is multiplied by the ratio field to create the "calibrated" half-hourly IMERG estimates. In V03 we found that the 1° GPCC data grid caused unphysical blockiness along coasts, so starting in V04 we trimmed the gauge contribution to the coast. Furthermore, the GPCC data volume adjustment caused blockiness over land, so it was removed. The net effect is to "spread" the gauge analysis precipitation values for a particular grid box to the surrounding grid boxes. To date, the resulting smoothing has not been considered a significant problem. Note that the zone outside the 60°N-S latitude band is only populated with gauge data and GPROF estimates in areas without snowy/icy surfaces, so the data coverage is not complete. Masking of snow/ice covered surfaces is performed using the Autosnow product. The satellite-gauge estimates are global, but not considered reliable over cold surface. Masking removes questionable GPROF estimates and allows IR-only estimates in the region 60º N-S.

3.9 POST-PROCESSING

IMERG ends with a precipitation post-processing step that introduces gauge information into the original multi-satellite-only half-hourly data (carried as field precipitationUncal). For the Final Run, the ratio between the monthly accumulation of half-hourly multi-satellite-only fields and the monthly satellite-gauge field is computed, then each half-hourly field of multi-satellite-only precipitation estimates in the month is multiplied by the ratio field to create the final half-hourly calibrated IMERG precipitation estimates.

The ratio between the monthly satellite-gauge and the monthly accumulation of half-hourly multi-satellite-only fields is limited to the range [0.2,3]. The cap of 3 was chosen because the value 2 (used in TRMM V6) was too restrictive. The value was moved to 3 because it did a better job of matching the two accumulations, while testing showed that 4 started introducing unrealistic shifts to the histogram of half-hourly precipitation rates for the month. Early in TRMM the lower bound was set to 0.5, but it can be argued that a smaller value allows matching between the two accumulations without creating the egregious high snapshot values that result when the upper bound is expanded too far.

The baseline IMERG near-real-time products follow the TMPA procedure in providing both the original multi-satellite estimate and a climatologically calibrated field. The climatological calibration is intended to make the near-real-time products as consistent as possible with the Final product. One important simplification compared to the TMPA is that both the DPR and CORRA-G are computed in real time for GPM. This contrasts to the situation in TRMM where the PR and TCI were not computed in real time and we have had to substitute TMI as the RT calibrator. Accordingly, in GPM we compute a straightforward calibration to the Final product using a climatological CORRA-G calibration. If the sub-monthly precipitation gauge combination option is incorporated in the Late product, presumably the need for post-processing will have to be re-assessed, but the Early product is certain to require the climatological calibration to the Final product. Note that this latency is not an issue in computing TMI-CORRA in the TRMM era retrospective processing.

3.10 PRECIPITATION PHASE

The precipitation phase, namely whether it is liquid, solid, or mixed, is not currently provided as a satellite-based calculation by the standard PMW precipitation algorithms, so we must use ancillary data sets to create the estimate. [Note: the DPR does estimate phase using the radar data.] Formally, there should be separate estimates for each phase. However, mixed-phase cases tend to be a small fraction of all cases, and we consider the estimation schemes to be sufficiently simplistic that estimating mixed phase as a separate class seems unnecessary. Some users need information on the occurrence of the solid phase, both due to the delays it introduces in moving precipitation water mass through hydrological systems, and due to the hazardous surface conditions that snow and ice create. Accordingly, we lump together liquid and mixed as "liquid" and compute a simple probability of liquid phase. [Note: a fraction is between 0 and 100% gives a probability that the precipitation is liquid; it does ***not*** denote a mixture in which the fraction gives the precipitation that is liquid and the converse of which is therefore solid. By far, the most likely event is either "all liquid" or "all solid", and the probability of each is the fraction and its converse, respectively.]

For the half-hourly data, we adopt the Liu scheme (personal communication, 2013; Sims and Liu 2015), which is under development for the Radiometer Team. The present (pre-publication) form is a simple look-up table for probability of liquid precipitation phase (PLPP) as a function of wet-bulb temperature, with separate curves for land and ocean. This is a current area of research, so we anticipate changes as research results are reported. Since this diagnostic is independent of the estimated precipitation, we choose to report the PLPP for all grid boxes, including those with zero estimated precipitation. [This raises the possibility that the IMERG PLPP field can be applied to any other global precipitation field for estimating phase.] The surface temperature, humidity, and pressure information needed to compute the surface wet-bulb temperature are taken from the JMA NWP forecast for the Early and Late Runs, and the ECMWF Interim reanalysis for the Final Run. These forecast and reanalysis fields are retrieved and reformatted by PPS.

GPROF2017 retrieves total hydrometeor mass in the atmospheric column (except the conical-scan imager PMW retrievals only consider total solid hydrometeor mass over land and coast and then implicitly correlate it to surface precipitation in any phase). Given these facts, the "precipitation" reported in this document refers to all forms of precipitation, including rain, drizzle, snow, graupel, and hail. The IR retrievals are calibrated to the passive microwave retrievals, again, without reference to precipitation phase. These IR calibrations are in-filled from surrounding areas in the snowy/icy-surface areas where PMW cannot provide estimates.

At the monthly scale the PLPP value could either be the fraction of the time that the precipitation is liquid or the fraction of the monthly accumulation that fell as liquid. The latter seems to be what most users will want, so this is the parameter computed. The monthly probability of liquid is the precipitation-rate-weighted average of all half-hourly probabilities in the month, except for grid boxes where zero precipitation is estimated for the month, in which case it is the simple average of all available probabilities in the month.

Note well that the assignment of phase does not change the units of precipitation, which is the depth of liquid. In the case of solid precipitation, this is usually referred to as snow water equivalent (SWE). The depth of fallen snow that corresponds to this SWE depends on the density of the snow. Typically, it takes about 10 mm of fallen snow to yield 1 mm of SWE, but the ratio depends on location, meteorological regime, time of year, and elevation. There is an excellent discussion of how Environment Canada is addressing this in Wang et al. (2017)..

3.11 ERROR ESTIMATES

Error estimates are a required item in the output datasets. The baseline fine-scale datasets errors are estimated following the TMPA downscaled monthly estimation scheme. The baseline monthly Final dataset error estimates are computed as part of the optimal estimation of the satellite-gauge combination. We expect that more sophisticated error fields will be incorporated as part of IMERG in the future, for example providing additional information on the error quantiles following Maggioni et al. (2014) or the correlation parameter computed in the Kalman filter methodology. In such a case, the critical problem is to limit the number of time/space-varying parameters that consequently require the insertion of additional parameter fields in each dataset.

3.12 QUALITY INDEX

Users recently requested a "simple" quality index to give some guidance on when they should most trust IMERG. While the goal is reasonable, there is no agreement about how this quantity should be defined. After some discussion within the team, two distinctly different quality indices were chosen for the half-hourly and monthly data fields for implementation in V05 (and continued in V06), summarized below. It is a matter of investigation to determine if users find these insightful, or if different quality indices should be developed for future releases. Details are provided in the document "IMERG Quality Index", available at *https://pmm.nasa.gov/sites/default/files/document_files/IMERG_QI.pdf* .

3.12.1 QIh: Quality Index for Half-Hourly Data

At the half-hourly scale, the best metric is some measure of the relative skill that might be expected from the fluctuating mix of different passive microwave- and infrared-based precipitation estimates. The Kalman smoother used in IMERG (and originated in the CPC Morphing [CMORPH] algorithm, Joyce et al. 2011) routinely recomputes estimates of correlation between GMI and each of the other satellite estimates in coarse blocks across the entire domain (90°N-S) and then uses these correlation coefficients (squared) to provide weights for use in the combination of forward-propagated passive microwave, backward-propagated passive microwave, and current-time infrared precipitation estimates. In V06 the polar caps have the same treatment without IR data. However, the formalism never provides an overall correlation for the combined estimate, so one approach is provided here.

The correlation coefficients developed for the Kalman smoother are substituted for inverse error variance to compute the approximate correlation coefficient of the merged precipitation estimate. Furthermore, the correlation coefficients are transformed with the Fisher (1915) z statistic before the computation and back-transformed afterwards, which is a simple variance stabilization transformation. Formally, the Fisher transformation requires that the two variables being correlated follow a bivariate normal distribution. While this is not true for precipitation, we adopt this approach as a first approximation to computing the correlation coefficient of the combined precipitation estimate because its use as a quality index seems reasonable and useful. The units are non-dimensional correlation coefficients.

There is one additional issue: we lack the zero half-hour correlation of each constellation member to the GMI for computational reasons in the current implementation of IMERG and need an approximate value. Lacking strong justification for alternatives, we chose to compute a set of baseline monthly zero hour correlations using the data span December 2014 – November 2015 from the Level 2 (GPROF) estimates after intercalibration. These baseline correlations are then dynamically adjusted based on nearby, in time, correlations. These are expected to be slightly

higher than if they had been computed from the zero half-hour outputs of the morphing scheme due to the lack of equivalent post-processing of the Kalman correlations.

3.12.2 QIm: Quality Index for Monthly Data

At the monthly scale, a relatively well-founded metric exists for random error, based on Huffman's (1997) analysis of sampling error for a particular data source for a month. The general form of the relationship is simplified to a relationship that can be inverted to give the number of samples. When all the constants on the right-hand side are set for the gauge analysis, but final satellite-gauge values are used for the estimated precipitation and random error values, the number variable is defined as the equivalent number of gauges. Following Huffman (1997), the interpretation is that this is the approximate number of gauges required to produce the estimated random error, given the estimated precipitation. The units are gauges per area, and in the current implementation the area is carried as 2.5°x2.5° of latitude/longitude, even though IMERG is computed on a much finer scale, in order to facilitate interpretation in large-error regions. Note that this formulation only addresses random error, not bias.

3.13 ALGORITHM OUTPUT

All output data files have multiple fields with PMM-mandated metadata and are written in HDF5, which is compatible with NetCDF4. All fields are produced for all data Runs. Table 3 lists the data fields. Recall that PMM provides an on-the-fly data subsetting by time, region, and parameter, so users are not required to download the entire file.

The output files for the various runs are identified with these prefixes (see *https://pmm.nasa.gov/sites/default/files/document_files/FileNamingConventionForPrecipitationProductsForGPMMissionV1.4.pdf*):

- 3B-HHR-E – half-hourly, Early Run
- 3B-HHR-L – half-hourly, Late Run
- 3B-HHR – half-hourly, Final Run
- 3B-MO – monthly, Final Run

As listed in Table 2, the notional requirement is that the output be on a global 0.1° grid. However, there is a strong argument that a fully global grid should be (approximately) equal-area, and this issue is under discussion within the project for future revisions. Also, the IR data are actually available on a 0.035° grid, and the question has been raised whether the notional grid size ought to be in the range 0.035°-0.05°. At present the baseline is left at 0.1° because there are scientific questions about downscaling microwave footprints to the finer scale, and operational questions about data volume.

3.14 PRE-PLANNED PRODUCT IMPROVEMENTS

Throughout the useful life of IMERG we plan for the code to be reasonably robust to errors, drop-outs, and changes in the make-up of the satellite constellation. The preceding discussion also detailed some developmental issues that are being addressed as we gain experience running IMERG. In addition, the team considers it helpful to pre-plan certain enhancements to the code that we are fairly certain will be required at some point.

Table 3. Lists of data field variable names and definitions to be included in each of the IMERG output datasets. Primary fields of interest to users are in italics.

Half-hourly data file (Early, Late, Final)	
precipitationCal	*Multi-satellite precipitation estimate with gauge calibration (recommended for general use)*
precpitationUncal	Multi-satellite precipitation estimate
randomError	*Random error for gauge-calibrated multi-satellite precipitation*
HQprecipitation	Merged microwave-only precipitation estimate
HQprecipSource	Microwave satellite source identifier
HQobservationTime	Microwave satellite observation time
IRprecipitation	IR-only precipitation estimate
IRkalmanFilterWeight	Weighting of IR-only precipitation relative to the morphed merged microwave-only precipitation
probabilityLiquidPrecipitation	*Probability of liquid precipitation phase*
PrecipitationQualityIndex	*Quality Index for precipitationCal field*
Monthly data file (Final)	
precipitation	*Merged satellite-gauge precipitation estimate (recommended for general use)*
randomError	*Random error for merged satellite-gauge precipitation*
gaugeRelativeWeight	Weighting of gauge precipitation relative to the multi-satellite precipitation
probabilityLiquidPrecipitation	*Accumulation-weighted probability of liquid precipitation phase*
PrecipitationQualityIndex	*Quality Index for precipitationCal field*

3.14.1 Addition/Deletion of Input Data

Satellites come and go over time. For the most part, satellite drop-outs, other than of the GPM Core itself, simply result in a smaller amount of input data for the system. Addition of data, on the other hand, is potentially complicated by a range of possible priorities and calibration needs of the new sensor. In IMERG we follow the work pioneered in the Version 7 TMPA, where extra satellite slots are programmed in, separated into conical and cross-track scanners. When a new sensor comes on-line, it can be assigned to an appropriate-type slot and start contributing from that point forward, once the calibration coefficients are determined, which can require several months of data. However, including the new sensor's data recorded before the date/time on which it is instituted in the dataset requires retrospective processing (next Subsection).

3.14.2 Upgrades to Input Data

When an existing sensor's data record is reprocessed, or a new sensor is introduced that has an archive not previously used, it is necessary to reprocess the archive of IMERG data to preserve consistent statistical behavior (to the extent possible) across the entire record. While reprocessing should not be undertaken lightly, given the computing demands on PPS and the disruption to the users, hard practical experience shows that we need to be more aggressive about this issue than has been the case previously for TMPA. For example, the second version of NESDIS AMSU, introduced in 2004, resulted in an underestimate of light rain. The result in TMPA during part of its Version 6 was a low bias in fractional coverage and rain amount over ocean. When an upgraded

version of the NESDIS AMSU was introduced in early 2007 these biases were greatly reduced, but we allowed the inhomogeneity to persist in the Version 6 TMPA archive. As a result, users had to be continually reminded that the relatively low values are a known problem, a problem that was not fixed until the Version 7 TMPA reprocessing some five years later.

3.14.3 Polar Sensors

The Multi-Satellite team has extended IMERG to the polar regions, consistent with GPM's fully global focus. The first step was to add PMW snapshot estimates to the HQ and merged data fields in V05, then we shifted to displacement vectors at higher latitudes by tracking TQV in MERRA-2 and GEOS-5 FP. These vectors morph the available high-latitude precipitation estimates in the backward/forward Kalman filter to compute the output estimates. In a future version, we will add available high-latitude estimates, including the TOVS and AIRS estimates computed using the Susskind et al. (1997) algorithm, and leo-satellite AVHRR IR (and other channel) estimates. This development work will require close cooperation with the experts in high-latitude GV.

3.14.4 Upgrades for Near-Real Time

It is likely that the Near-Real Time products will require modifications to create the most useful output. For example, we started with somewhat loose latency limits for the Early and Late Runs and pared back the timing as we gained experience with the realities of the data reception. For the Late Run, this requires balancing the useful time range of backward-propagated microwave data against the latency of the following microwave overpass. If the daily gauge option is instituted for the Late Run, we believe we can fit it into the latency structure of the baseline scenario. That is, if the daily gauge analysis has a latency that is much longer than the Late Run satellites require, the daily gauge computation might be able to use the PDF of data up through the previous day.

3.14.5 Use of Model Estimates

Validation work by Ebert et al. (2007) and Gehne et al. (2016) among others, demonstrates that numerical model estimates of precipitation can out-perform observational estimates at daily 0.25°x0.25° scale in the cool season over land. This stands in contrast to the poor performance by model estimates in tropical and subtropical conditions for day-to-day variations, diurnal cycle, and seasonal variation. The Multi-Satellite team's experience in isolating bias in input datasets and the flexible, error-sensitive behavior of the Kalman filter concept seem to suggest that IMERG is a natural platform for testing the joint use of observational and model-based precipitation estimates. This is particularly true given that IMERG is now extended into polar regions (Subsection 3.14.3). It is absolutely clear that the team intends to maintain a robust observation-only capability throughout GPM to support a variety of applications, not the least being validation of model estimates. However, a parallel joint observation-model product is a worthy contribution to the project and to advancing scientific understanding and societal benefit applications.

3.15 OPTIONS FOR PROCESSING

Since the clear mandate for the Day-1 IMERG algorithm was driven by a very aggressive schedule, the baseline algorithm was designed around code that was already running and tested. At the same time, the team had several concepts in research that might become sufficiently mature that one or more of them might be prime targets for upgrading the future versions.

3.15.1 Use of Multi-Spectral Geo-Data

Besides the thermal IR channel discussed above, geo-satellites also provide other channels, usually visible and one or more spread across the IR spectrum. Historically, these channels have not been

used due to apparent modest improvements in skill, difficulties in handling the higher data volumes, and limitations to daylight hours (for visible). However, our ongoing dependence on geo-satellite data to fill large gaps between PMW overpasses and the increasing number of (non-microwave) channels on newer satellites make it important to reconsider this aspect. Recent studies seem to indicate reasonable increases in skill using modern neural net approaches, particularly when visible data are used (Behrangi et al. 2009). Several important steps must be taken to capitalize on this apparent benefit in using multi-spectral data. First the scientific development must be advanced to operational status. Second, we must work with the data providers to arrange for routine delivery of the data in a useful format, including a complete archive. Third, choices must be made on the selection of channels, recognizing that previous generations of geo-satellites had less-capable sensors than those now in use.

3.15.2 Incorporating Cloud Development Information

Precipitation develops and decays over time periods that are short compared to the typical revisit time of the leo-PMW constellation. As noted above, the autocorrelation of observed and propagated precipitation fields may drop from 1.0 to ~0.6 within 30 minutes and further fall to ~0.4 or lower after an hour of propagation, while instantaneous geo-IR precipitation estimates are notoriously poor, but nonetheless provide a minimum floor of skill when a gridbox lacks recent propagated leo-PMW estimates. Taking a different approach, capturing the dynamic evolution of geo-IR cloud images may help to identify cloud systems in various stages of development. This approach to addressing the "cloud development problem" is a relatively new area of research and requires further investigation to determine the best strategies for capturing the development process. One possibility is to drive a highly simplified conceptual cloud model with parameters computed from the geo-IR Tb data, as in the Bellerby et al. (2009) Lagrangian Model (LMODEL). Another is to modify the propagated leo-PMW precipitation estimates with time based on parameters computed from the geo-IR Tb data, as in the Behrangi et al. (2010) Rain Estimation using Forward Adjusted-advection of Microwave Estimates (REFAME).

3.15.3 Use of Daily Gauges

The biases discussed previously vary on sub-monthly time scales, of course. To address this problem, we will examine the possibility of refining the bias correction approach described in Subsection 3.8 through the use of daily gauge analysis. CPC has developed a new technique to correct the bias in high-resolution satellite precipitation estimates through matching the PDF of the satellite estimates against that of the daily gauge analysis (Xie et al. 2010). The PDF bias correction is carried out in two steps using historical, and then real-time data. First, PDF tables are constructed for each 0.25° lat/lon gridbox over the global land and for each calendar day using co-located satellite and gauge data pairs over a spatial domain centered on the target grid box and over a sliding window of 31 days centered on the target calendar day for the 16-year period beginning in 1998. The spatial domain is expanded until a sufficient number of data pairs are collected. After the correction using historical data, the satellite estimates are further calibrated against the real-time data to remove the year-to-year variations in the bias. To this end, PDF tables are created using co-located data collected over a 30-day period ending at the target date. The least numbers of co-located data pairs used in Xie et al. (2010) to create PDFs for the corrections are 500 and 300 using historical and real-time data, respectively.

3.15.4 Improve Error Estimation

Error estimation has proved resistant to easy progress, in no small part because precipitation is a highly intermittent, non-negative process resulting in non-Gaussian, strongly skewed PDF's of precipitation events that are generated at very fine space and time scales, and which demonstrate

multi-scale correlation structures. The current scheme for computing half-hourly random error estimates is based on the Huffman (1997) approach for monthly data, and badly needs to be replaced. The Precipitation Uncertainties for Satellite Hydrology (PUSH) scheme (Maggioni et al. 2014) seems to promise a clean computation of the full quantiles of precipitation for each grid box, which presumably encompasses both systematic and random error. Detailed work on PUSH is being led by Dr. Maggioni under separate funding, so the role of the present project is to work with her group and make use of the results as feasible. Another promising concept developed under separate funding is the Probabilistic QPE using Infrared Satellite Observations (PIRSO; Kirstetter et al. 2018). Despite the name, it should be applicable to IMERG. Note that neither scheme directly addresses the grand challenge of accounting for the time/space error correlation structure in estimating error for arbitrary time/space averages of IMERG data.

4. TESTING

The CMORPH-KF and PERSIANN-CCS systems were brought up in the GSFC development environment in GSFC Code 612 with the minimum number of changes possible to ensure that the code as originally presented was functional. The TMPA code already satisfied this requirement. Thereafter, the IMERG code was the development system.

4.1 ALGORITHM VERIFICATION IN THE PPS SYSTEM

As each generation of IMERG code is developed, it is validated on the development system. At the agreed-upon deliveries the entire package is assembled and transferred to PPS for integration and testing. This allows us to validate the PPS processing. The IMERG products are compared against coincident CMORPH-KF, PERSIANN-CCS, TMPA, prior IMERG, and various ground validation fields. The goal in this stage is to shake out as many bugs and conceptual difficulties as possible, applying corrections to the production and near-real-time IMERG instantiations.

4.2 ALGORITHM VERIFICATION FOR THE DIFFERENT RUNS

The main features to be validated between the near-real-time and production instantiations are the use of somewhat different input data sets and the addition of monthly gauge calibration in the Final run. As before, it is important to compare the results to the other estimates and validation data listed above.

4.3 ALGORITHM VALIDATION

The more formal algorithm validation is examining various aspects of the IMERG results. At the snapshot level, comparison to the fine-scale NOAA Multi-Radar Multi-Sensor (MRMS) analyses, and to the PMM Kwajalein radar archives are considered key. As part of this effort, we carry out similar comparisons against the gridded Level 2 input data. The performance at larger space-time scales is being assessed using accumulations of these three datasets, as well as the CPC daily gauge analysis, the IPWG validation sites (Australia, CONUS, Japan, South America, Western Europe), the GPCC global monthly gauge analysis, the Pacific atoll data, and the ATLAS II buoy data. For higher-latitude validation, the GPCC data can be used to validate the satellite-only products. The team already has access to Finnish Meteorological Institute precipitation gauge data, and performance in Alaska is the topic of thesis work at U. of Utah. At a minimum, metrics include bias, root-mean-square error, mean absolute error, correlation, and skill scores. Decompositions into hit error, miss error, etc. following Tian et al. (2009) are considered as well. We are working

with the validation teams to examine the IMERG datasets with the detailed validation approaches that they manage. Finally, we work with selected users, particularly hydrologists, to incorporate the test datasets and report their experiences to help determine what IMERG's level of skill is for their applications. Some early V06 results are displayed in the release notes, posted at

https://pmm.nasa.gov/sites/default/files/document_files/IMERG_V06_release_notes.pdf

and this discussion will be expanded as additional results are computed.

5. PRACTICAL CONSIDERATIONS

5.1 MODULE DEPENDENCIES

The baseline structure of IMERG is shown in Fig. 2. We have not enforced consistency on the various boxes in the sense that some boxes might be programmed as multiple modules, while others will be computed in a single module. As summarized in Subsection 5.2, the data flow between modules, and between executions of the same module, is carried out using files, which typically have fixed names. Input and output datasets necessarily have names that reflect the time sequencing of the data that they contain.

5.1.1 Calibrations

The satellite-satellite calibrations, which include the PMW intercalibrations to a TRMM/GPM standard (block 2), IR-PMW precip calibration for the IR estimates (block 10), and the Kalman filter weights (block 6), are conceptually asynchronous with the actual half-hourly precipitation dataset processing. It is a matter of computational choice within PPS as to whether the calibrations are run sequentially or in parallel, but the system is designed to be very forgiving of occasional missed calibration match-ups – without significant loss of skill it can run with the then-current calibration files, as long as the dropouts do not become too severe. The heritage TMPA system computed the PMW intercalibration on a calendar month basis, while the PERSIANN-CCS and CMORPH-KF run the IR-PMW and KF weights, respectively, on trailing accumulations of match-ups. For IMERG we necessarily run all the Early and Late calibrations on trailing accumulations of match-ups. The post-real-time Final run has to wait for the GPCC precipitation gauge analysis and the ECMWF ancillary data, so we accumulate the match-ups with a sufficient delay after real time that the Final calibrations are approximately centered, with the exception of the Kalman statistics, which consist of the current and previous two months of data.

The only important difference between near- and post-real-time runs comes in the last calibration, which is computed for the near-real-time as climatological adjustments to the Final product, and for the post-real-time as calendar-month adjustments to, and combination with monthly gauge analyses.

As noted above, we compute three runs of the algorithm, namely the "Early", "Late", and "Final" Runs at about 4 hr, 14 hr, and 3.5 months after observation time. The simplest approach is chosen, namely to maintain three entirely separate sets of files and to compute everything in each run. This eliminates dependencies between runs and facilitates retrospective processing.

5.1.2 Parallelization

The forward V05 retrospective processing revealed that the original CMORPH-KF propagated time series was programmed to be efficient in computational resources but required serial processing. This constituted significant impediment to timely completion for a long record. Thus, in V06 the forward propagated time series of PMW was re-worked to be computed from scratch for each half hour. Taking a cue from the backward propagation, which of necessity is recomputed anew for each half hour, the HQ data in the previous 7 hours is used to develop the forward-propagated PMW field, since the KF correlations beyond 7 hours are negligible. While less efficient than the original scheme, the shift allows parallel computation for each half hour's forward propagation and significantly decreases wall clock time.

AS well, the rotating accumulation files used for calibration impose a serial requirement. It is possible to have several "chunks" of years, each starting from scratch and just filling accumulation files until they are "full", then computing results. This would allow a coarse-scale parallelization that could reduce reprocessing wall clock time by a factor of the number of chunks (plus extra overhead).

5.2 FILES USED IN IMERG

Input, output, inter-module data transfer, and inter-run/static data storage is accomplished through files in IMERG. Table 4 displays our best estimate of what the file sizes and count are, but some of the file sizes are variable due to internal compression. It is important to note that the granularity of the input data implies that two of each of the input types will have to be used in each half-hour with fair regularity. On the other hand, the precipitation gauge analysis provides only one file in a month, which is also true for the monthly Merged Satellite/Gauge product. Several of the options and planned upgrades will require the use, transport, and accumulation of data in additional files.

5.3 BUILT-IN QUALITY ASSURANCE AND DIAGNOSTICS

To the extent possible, every effort is being made to incorporate quality assurance checks in the IMERG system. This includes quality checks of all input data, and of selected intermediate and output data based on metrics developed for TRMM. The goal of these metrics is to capture discrepancies before they propagate into the downstream processing. PPS toolkit warning and error messages are the primary mechanism used to flag potential problems. Optional diagnostic information are available to the operator when requested. It is possible that a separate, post-processing algorithm will be used to extend the quality assurance procedure to the Final product as part of the operational development. The goal of this post-processing algorithm would be to capture more subtle issues than observable during production.

5.4 SURFACE TEMPERATURE, RELATIVE HUMIDITY, AND PRESSURE DATA

The estimation of precipitation phase requires global surface temperature, relative humidity, and surface pressure data, since the operational algorithms cannot provide phase directly. The JMA model forecast and GANAL analysis data are computed in 6-hour increments, and five 6-hour increments are provided within a single delivered file (i.e., a day). The data are provided in grib2 format, and converted to individual 6-hour files in flat binary by PPS using the standard wgrib2 utility. The ECMWF model data are computed in 3-hour increments and converted from grib2 format to binary. These binary files are read into IMERG and the appropriate parameters extracted and used to compute the percent probability of liquid phase.

Table 4. Estimates of file counts and sizes used in IMERG for the entire TRMM-GPM era. The letters i, o, t, a, s in "Module Relation" indicate input, output, transfer (between modules or within a module), accumulator, and static, respectively. The numbers in "Module Relation" are keyed to the numbered boxes in Fig. 2. M-T MADRAS is not included in this list due to its short, gappy record.

INTERMEDIATE/STATIC				
ID	*# Files*	*Size (MB)*	*Total Size (MB)*	*Module Relation*
GMI-CORRA accum	1	1385	1385	a2
GMI-other cal	21	25	525	s2
Surface type	1	52	52	s2
TMI-CORRA accum	1	1385	1385	a2
TMI-other cal	21	25	525	s2

INPUT					
ID	*# Granules*	*Granularity*	*Granule Size (MB)*	*Total Size (MB)*	*Module Relation*
AIRS	1	One orbit	11	11	i2
AMSR x 2	2	One orbit	56	112	i2
AMSU x 3	3	One orbit	56	168	i2
ATMS x 2	2	One orbit	56	112	i2
CrIS	1	One orbit	11	11	i2,i4
GMI-CORRA	1	One orbit	328	328	i2
GEOS-5 FP	1	One hour	9	9	i4
GMI	1	One orbit	56	56	i2
GPCC	1	One month	8	8	i11
IR	2	One hour	65	130	i1,t1-4,t1-8
JMA Forecast Tsfc, RHsfc, Psfc	1	forecast run	121	121	i11,i12
JMA Analysis Tsfc, RHsfc, Psfc	1	analysis run	120	120	i11,i12
MERRA-2	1	One day	60	60	i4
MHS x 5	5	One orbit	56	280	i2
SAPHIR	1	One orbit	56	56	i2
SSMI x 3	3	One orbit	56	168	i2
SSMIS x 4	4	One orbit	56	224	i2
TMI-CORRA	1	One orbit	328	328	i2
TMI	1	One orbit	56	56	i2
TOVS	1	One orbit	11	11	i2

OUTPUT					
ID	*# Granules*	*Granularity*	*Granule Size (MB)*	*Total Size (MB)*	*Module Relation*
Half-hourly IMERG	1	30 minutes	181	181	o11,o12
Monthly IMERG (Final Run only)	1	One month	58	58	o11

Table 4, cont.

TRANSFER					
ID	*# Granules*	*Granularity*	*Granule Size (MB)*	*Total Size (MB)*	*Module Relation*
Gridded HQ	14*	One orbit	103	1442	t2
TMI-CORRA cal	1	One orbit	259	259	t2
GMI-CORRA cal	1	One orbit	259	259	t2
Cloud Motion Vectors	2	One hour	0.2	0.4	t4,t4-6
Kalman Filter weights	1	One month	290	290	t6-7
PMW	2	30 minutes	103	206	t2-5,t2-5,t2-9
PMW forward and backward prop	2	30 minutes	103	206	t5-7
Intermediate IR	1	30 minutes	65	65	t8
Intermediate HQ	1	30 minutes	103	103	t9
TQV sub areas	1	30 minutes	79	79	t8
CCS precip sub areas (unadjusted)	1	30 minutes	54	54	t8-10
CCS precip sub areas (adjusted)	1	30 minutes	54	54	t10
Cloud classification	48	30 minutes	0.4	19.2	s8
IR/rainrate	48	30 minutes	14	672	s8
CCS global precip (adjusted)	1	30 minutes	54	54	t10-6,t10-7
Merged PMW/IR (uncal)	1	30 minutes	103	103	t7-11,t7-12

* Although 34 sources of "high-quality" satellite data are listed under "INPUT", it is assumed that no more than 14 such satellites will be available at any given time.

5.5 EXCEPTION HANDLING

Like the TMPA predecessor, the IMERG system is quite robust in handling exceptions, including input file existence and integrity, command-line consistency, and routine data checks. It is the responsibility of the Multi-Satellite Team to create and update the toolkit error messages. When issues are flagged by the toolkit, additional diagnostic output is integrated into the code by the developers to assist in isolating the problem when requested by the operator by setting the "debug" flag. Error reporting is used when exceptions are significant enough to halt execution. Warning reporting is used when exceptions should be noted, but processing can continue. In both cases, PPS contacts the algorithm developers to determine the severity of the exception and how best to address it.

5.6 TRANSITIONING FROM TMPA TO IMERG PRODUCTS

During the start-up testing described in Section 4, we provided routinely computed IMERG products to successively more users as soon as practical in order to 1) gain critical feedback from key user groups as early as possible, and 2) give users the maximum time possible to make the transition to the new processing paradigm. This occurred in late 2014, clearly using a short (6-9 month) GPM record as the calibrator to generate V03 "Day-1" products. Even as V03, V04, V05,

and V06 processing for IMERG products are carried out, the TMPA products are continuing to be produced to support users who require the long record that the TMPA and TMPA-RT provide. The first retrospective processing for IMERG through the TRMM era (nominally starting in 1998, but initially starting in June 2000), is expected to occur in Spring 2019, using IMERG V06 code to create the final TRMM Version 8 data sets. The TMPA products will continue to be produced for a few additional months to allow a graceful transition. This foresees a shutdown of TMPA processing in Fall 2019. Note that TMPA-RT has long used climatological TRMM-based RT calibrations, so the only actual effect of the end of TRMM is the loss of the TMI precipitation estimates in April 2015 in the combined microwave field. The impact on the final TMPA was more serious, since it routinely used the TCI product as a calibrator. When the PR no longer produced useful estimates, in October 2014, we implemented a climatological calibration and accepted the lower quality result in order to maintain continuity. Should too many legacy sensors cease providing data, the TMPA legacy products could degrade to the point that we might choose to end production less gracefully. See *https://pmm.nasa.gov/sites/default/files/document_files/TMPA-to-IMERG_transition_190313*.pdf .

5.7 TIMING OF RETROSPECTIVE PROCESSING FOR IMERG PRODUCTS

As hinted in the previous Subsection, the decision to retrospectively process the IMERG archive as the result of algorithm changes in one or more input products critically depends on the availability of a completely reprocessed archive of the affected input product(s). In particular, when a general reprocessing is called for in the GPM suite of products, the IMERG products can be started only after the requisite Level 2 GPM products have been finalized and substantially reprocessed, allowing IMERG to apply the upgraded data for calibration and routine use in the products.

6. ASSUMPTIONS AND LIMITATIONS

6.1 DATA DELIVERY

In general, the IMERG package is extremely forgiving of dropouts in individual sensors, including the calibrating sensor products and the geo-IR data. Our experience with IMERG is that extended drop-outs are rare for the GMI and DPR (and so CORRA-G), but serious dropouts have occurred for partner satellites and ancillary data.

6.2 ASSUMED SENSOR PERFORMANCE

The implicit assumption in the IMERG code is that the various PMW datasets are either stable or unavailable. The main impact of data denial is on IMERG quality due to longer runs of morphed data and more-frequent use of IR estimates. What about changes in sensor performance? There is a time-dependent calibration update for the IR-PMW and GMI-CORRA calibrations in both near-real and post-real time. [For the TRMM era, TMI-TCI was stable.] So, if the IR or GMI is drifting, the time-dependent calibrations should account for the problem. However, using climatological GMI-to-everything-else calibrations means a drifting GMI cannot be accommodated. We would be more flexible if we decide to routinely update these GMI-to-everything-else calibrations, since drift in the GMI would be automatically accommodated, but such a modification would require a major development effort. For all sensors, including geo-IR

and gauge, variations in the amount of unbiased noise should not automatically bias the results, although the resulting random errors will fluctuate correspondingly.

7. REFERENCES

Adler, R.F., G.J. Huffman, A. Chang, R. Ferraro, P. Xie, J. Janowiak, B. Rudolf, U. Schneider, S. Curtis, D. Bolvin, A. Gruber, J. Susskind, P. Arkin, E.J. Nelkin, 2003: The Version 2 Global Precipitation Climatology Project (GPCP) Monthly Precipitation Analysis (1979-Present). *J. Hydrometeor.*, **4**(6), 1147-1167.

Adler, R.F., M. Sapiano, G.J. Huffman, J.-J. Wang, G. Gu, D.T. Bolvin, L. Chiu, U. Schneider, A. Becker, E.J. Nelkin, P. Xie, R. Ferraro, D.-B. Shin, 2018: The Global Precipitation Climatology Project (GPCP) Monthly Analysis (New Version 2.3) and a Review of 2017 Global Precipitation. *Atmos.*, **9**(4), 14 pp. *doi:10.3390/atmos9040138*

Behrangi, A., K. Hsu, B. Imam, S. Sorooshian, G.J. Huffman, R.J. Kuligowski, 2009: PERSIANN-MSA: A Precipitation Estimation Method from Satellite-based Multi-spectral Analysis. *J. Hydrometeor.*, **10**(6), 1414-1429.

Behrangi, A., B. Imam, K. Hsu, S. Sorooshian, T.J. Bellerby, G.J. Huffman, 2010: REFAME: Rain Estimation Using Forward Adjusted-Advection of Microwave Estimates. *J. Hydrometeor.*, **11**, 1305-1321.

Behrangi, A., G. Stephens, R.F. Adler, G.J. Huffman, B. Lambrigtsen, M. Lebsock 2014: An Update on Oceanic Precipitation Rate and Its Zonal Distribution in Light of Advanced Observations from Space. *J. Climate*, **27**, 3957-3965. *doi:10.1175/JCLI-D-13-00679.1*

Bellerby, T., K. Hsu, S. Sorooshian, 2009: LMODEL: A Satellite Precipitation Methodology Using Cloud Development Modeling. Part I: Algorithm Construction and Calibration. *J. Hydrometeor.*, **10**, 1081-1095.

Bosilovich, M. G., R. Lucchesi, M. Suarez, 2016: MERRA-2: File Specification. GMAO Office Note No. 9 (Version 1.1), 73 pp, available from *https://gmao.gsfc.nasa.gov/pubs/docs/Bosilovich785.pdf*

Ebert, E.E., J.E. Janowiak, C. Kidd, 2007: Comparison of Near-Real-Time Precipitation Estimates from Satellite Observations and Numerical Models. *Bull. Amer. Meteor. Soc.*, **88**, 47-64.

Fuchs, T., J. Rapp, F. Rubel, B. Rudolf, 2001: Correction of Synoptic Precipitation Observations due to Systematic Measuring Errors with Special Regard to Precipitation Phases. *Phys. Chem. Earth (B)*, **26**, 689-693.

Gehne, M., T.M. Hamill, G.N. Kiladis, K.E. Trenberth, 2016: Comparison of Global Precipitation Estimates across a Range of Temporal and Spatial Scales. *J. of Climate*, **29**, 7773-7795.

Gelaro, R., W. McCarty, M.J. Suárez, R. Todling, A. Molod, L. Takacs, C.A. Randles, A. Darmenov, M.G. Bosilovich, R. Reichle, K. Wargan, L. Coy, R. Cullather, C. Draper, S. Akella, V. Buchard, A. Conaty, A.M. da Silva, W. Gu, G.-K. Kim, R. Koster, R. Lucchesi, D. Merkova, J.E. Nielsen, G. Partyka, S. Pawson, W. Putman, M. Rienecker, S.D. Schubert, M. Sienkiewicz, B Zhao, 2017: The Modern-Era Retrospective Analysis for Research and Applications, Version 2 (MERRA-2). *J. Climate.*, **30**, 5419–5454. *doi:10.1175/JCLI-D-16-0758.1*.

Kidd, C., 2018: Algorithm Theoretical Basis Document (ATBD) Version 01-02 for the NASA Global Precipitation Measurement (GPM) Precipitation Retrieval and Profiling Scheme (PRPS). GPM Project, Greenbelt, MD, 16 pp. *https://pps.gsfc.nasa.gov/Documents/20180203_SAPHIR-ATBD.pdf*

Hong, K.L. Hsu, S. Sorooshian, X. Gao, 2004: Precipitation Estimation from Remotely Sensed Imagery Using an Artificial Neural Network Cloud Classification System. *J. Appl. Meteorol.*

43, 1834–1852.

Huffman, G.J., R.F. Adler, D.T. Bolvin, G. Gu, E.J. Nelkin, K.P. Bowman, Y. Hong, E.F. Stocker, D.B. Wolff, 2007: The TRMM Multi-satellite Precipitation Analysis: Quasi-Global, Multi-Year, Combined-Sensor Precipitation Estimates at Fine Scale. *J. Hydrometeor.*, **8**, 38-55.

Huffman, G.J., R.F. Adler, M. Morrissey, D.T. Bolvin, S. Curtis, R. Joyce, B McGavock, J. Susskind, 2001: Global Precipitation at One-Degree Daily Resolution from Multi-Satellite Observations. *J. Hydrometeor.,* **2**(1), 36-50.

Joyce, R.J., P. Xie, J.E. Janowiak, 2011: Kalman Filter Based CMORPH. *J. Hydrometeor.*, **12**, 1547-1563. *doi:10.1175/JHM-D-11-022.1*

Kirstetter, P.-E., N. Karbalaee, K. Hsu, Y. Hong, 2018: Probabilistic Precipitation Rate Estimates with Space-based Infrared Sensors. *Quart. J. Roy. Meteor. Soc.***,** 144, 192-205. *doi:10.1002/qj.3243*

Krajewski, W.F., J.A. Smith, 1991: On the Estimation of Climatological Z–R Relationships. *J. Appl. Meteor.*, **30**, 1436–1445.

Legates, D.R., 1987: *A Cimatology of Global Precipitation Publications in Climatology*, **Vol. 40**, Univ. of Delaware, 85 pp.

Legates, D.R., C.J. Willmott, 1990: Mean Seasonal And Spatial Variability In Gauge-Corrected, Global Precipitation. *Internat. J. Climatol.*, **10**, 111-127.

Lucchesi, R., 2017: File Specification for GEOS-5 FP. GMAO Office Note No. 4 (Version 1.1), 61 pp, available from https://gmao.gsfc.nasa.gov/products/documents/GEOS_5_FP_File_Specification_ON4v1_1.pdf.

Maggioni, V., M.R.P. Sapiano, R.F. Adler, Y. Tian, G.J. Huffman, 2014: An Error Model for Uncertainty Quantification in High-Time Resolution Precipitation Products. *J. Hydrometeor.*, **15**(3), doi:10.1175/JHM-D-13-0112.1, 1274-1292.,

Meng, H., B. Yan, R. Ferraro, C. Kongoli, 2012: Snowfall Rate Retrieval Using Passive Microwave Measurements. 12th Specialist Meeting on Microwave Radiometry and Remote Sensing of the Environment, 5-9 March 2012, Frascati, Italy.

Miller, J.R., 1972: A Climatological Z-R Relationship for Convective Storms in the Northern Great Plains. *15th Conf. on Radar Meteor.*, 153-154.

Romanov, P., 2016: Global 4km Multisensor Automated Snow/Ice Map (GMASI) Algorithm Theoretical Basis Document. NOAA NESDIS Cent. for Sat. Appl. and Res., 61 pp. http://www.star.nesdis.noaa.gov/smcd/emb/snow/documents/Global_Auto_Snow-Ice_4km_ATBD.pdf

Schneider, U., A. Becker, P. Finger, A. Meyer-Christoffer, M. Ziese, B. Rudolf, 2014: GPCC's New Land-surface Precipitation Climatology based on Quality-controlled In-situ Data and its Role in Quantifying the Global Water Cycle. Theor. Appl. Climatol., 115, 15-40. *doi:10.1007/s00704-013-0860-x . http://link.springer.com/article/10.1007%2Fs00704-013-0860-x*

Schneider, U., P. Finger, A. Meyer-Christoffer, M. Ziese, A. Becker, 2018: Global Precipitation Analysis Products of the GPCC. GPCC Internet Publication, DWD, 17 pp. Available online at *ftp://ftp-anon.dwd.de/pub/data/gpcc/PDF/GPCC_intro_products_2008.pdf*.

Sevruk, B., 1989: Reliability of Precipitation Measurements. *Proc. WMO/IAHS/ETH Workshop on Precipitation Measurements*, St. Moritz, Switzerland, World Meteor. Org., 13–19.

Sims, E.M., and G. Liu, 2015: A Parameterization of the Probability of Snow–Rain Transition. *J. Hydrometeor.*, **16**, 1466–1477. *doi:10.1175/JHM-D-14-0211.1*

Susskind, J., P. Piraino, L. Rokke, L. Iredell, A. Mehta, 1997: Characteristics of the TOVS Pathfinder Path A dataset. *Bull. Amer. Meteor. Soc.,* **78,** 1449–1472.

Tian, Y., C. Peters-Lidard, J. Eylander, R. Joyce, G. Huffman, R. Adler, K.-L. Hsu, F. J. Turk, M. Garcia, J. Zeng, 2009: Component Analysis of Errors in Satellite-Based Precipitation Estimates. *J. Geophys. Res, - Atmos*., **114**, D22104.

Villarini, G., P.V. Mandapaka W.F. Krajewski, R.J. Moore, 2008: Rainfall and Sampling Errors: A Rain Gauge Perspective. *J. Geophys. Res*., **113**, D11102, *doi:10.1029/2007JD009214*.

Wang, X.L., H. Xu, B. Qian, Y. Feng, E. Mekis, 2017: Adjusted Daily Rainfall and Snowfall Data for Canada. *Atmos.-Ocean*, **55**, 155-168. *doi:10.1080/07055900.2017.1342163*

Xie, P., S.-H. Yoo, R. Joyce, Y. Yarosh, 2010: A High-Resolution Gauge-Satellite Merged Global Precipitation Analysis and Its Applications for Model Verifications. *WMO 3rd Internat. Conf. on QPE / QPF and Hydrol.*, 18-22 October, 2010, Nanjing, China.

8. ACRONYMS

AIRS	Advanced Infrared Sounder
AMSR[E,-2,-3]	Advanced Microwave Scanning Radiometer [Earth Observing System, 2, 3]
ATBD	Algorithm Theoretical Basis Document
ATMS	Advanced Technology Microwave Sounder
AVHRR	Advanced Very High Resolution Radiometer
CLIMAT	Monthly Climatological Data
CMORPH-KF	CPC Morphing – Kalman Filter technique
CONUS	CONtiguous U.S.
CPC	Climate Prediction Center
CPO	Climate Program Office
CORRA[-G,-T]	Combined Radar-Radiometer Algorithm [specifically for GPM, TRMM]
CrIS	Cross-track Infrared Sounder
CRU	Climate Research Unit
DISC	Data and Information Services Center
DMSP	Defense Meteorological Satellite Program
DPR	Dual-frequency Precipitation Radar
DWD	Deutscher Wetterdienst
ECMWF	European Centre for Medium-range Weather Forecasting
EUMETSAT	European organization for the exploitation of Meteorological Satellites
FAO	Food and Agriculture Organization
GCOMW	Global Change Observation Mission - Water
geo	geosynchronous Earth orbit
GEOS-5	Goddard Earth Observing System model, Version 5
GEOS FP	Goddard Earth Observing System Forward Processing
GESDISC	Goddard Earth Science Data and Information System Center
GIOVANNI	Geospatial Interactive Online Visualization ANd aNalysis Infrastructure
GEWEX	Global Energy and Water cycle Experiment
GHCN	Global Historical Climatology Network
GMI	GPM Microwave Imager
GMS	Geosynchronous Meteorological Satellite
GOES	Geosynchronous Operational Environmental Satellite
GOSAT	Greenhouse gases Observing SATellite
GPCC	Global Precipitation Climatology Centre
GPCP	Global Precipitation Climatology Project
GPM	Global Precipitation Measurement mission

GSFC	Goddard Space Flight Center
G-WADI	Water and Development Information for Arid Lands – a Global Network
HDF	Hierarchical Data Format
IMERG	Integrated Multi-satellitE Retrievals for GPM
IR	Infrared
JMA	Japanese Meteorological Agency
JPSS	Joint Polar Satellite System
KF	Kalman filter version
leo	low Earth orbit
LMODEL	Lagrangian Model
LT	Local Time
MADRAS	Microwave Analysis and Detection of Rain and Atmospheric Structures
MERRA-2	Modern-Era Retrospective analysis for Research and Applications, Version 2
Meteosat	Meteorological Satellite
METOP[-SG]	Meteorological Polar Orbit satellite [Second Generation]
MHS	Microwave Humidity Sounder
MIS	Microwave Imager Sensor
MRMS	(NOAA) Multi-Radar Multi-Sensor (precipitation analysis)
MTSat	Multi-functional Transport Satellite
MWI	Microwave Imager
MWS	Microwave Sounder
NASA	National Aeronautics and Space Administration
NCEI	National Centers for Environmental Information (formerly NCDC, which still appears in the NCEI URLs)
NESDIS	National Environmental Satellite Data and Information Service
NetCDF	Network Common Data Format
NEWS	NASA Energy and Water Studies program
NOAA	National Oceanic and Atmospheric Administration
NRT	Near Real Time
NSF	National Science Foundation
PDF	Probability Density Function
PERSIANN-CCS	Precipitation Estimation from Remotely Sensed Information using Artificial Neural Networks – Cloud Classification System
PLPP	Probability of Liquid Phase Precipitation
PMM	Precipitation Measurement Missions
PMW	Passive Microwave
PPS	Precipitation Processing System
PR	Precipitation Radar
PRECTOT	Total precipitation from atm model physics (surface precipitation rate)
REFAME	Rain Estimation using Forward Adjusted-advection of Microwave Estimates
RT	Real Time
SAHRA	Sustainability of semi-Arid Hydrology and Riparian Areas
SNPP	Suomi National Polar-orbiting Partnership
SSMI	Special Sensor Microwave Imager
SSMIS	Special Sensor Microwave Imager/Sounder
SYNOP	Synoptic Weather Report
TCI	TRMM Combined Instrument product
TMI	TRMM Microwave Imager

TMPA	TRMM Multi-satellite Precipitation Analysis
TOVS	Television-Infrared Observation Satellite (TIROS) Operational Vertical Sounder
TQI	Total precipitable ice water
TQL	Total precipitable liquid water
TQV	Total precipitable water vapor
TRMM	Tropical Rainfall Measuring Mission
UNESCO	United Nations Educational Scientific and Cultural Organization
URL	Universal Resource Locator (usually the web address)
USWRP	U.S. Weather Research Program
UTC	Universal Coordinated Time
Version 6, 7, 8	TRMM version numbers (note well the single digit)
V03, V04, V05, V06	GPM version numbers (note well the leading zero digit)
WSF-M	(DoD) Weather Satellite Follow-on - Microwave
3B-HHR-E	half-hourly gridded precipitation estimate, Early Run
3B-HHR-L	half-hourly gridded precipitation estimate, Late Run
3B-HHR	half-hourly gridded precipitation estimate, Final Run
3B-MO	monthly gridded precipitation estimate, Final Run